

## Thermal Equilibrium

$$\text{Heating} = \text{Cooling} \Rightarrow T$$

$T$ : the temperature in the Maxwellian distribution of thermal velocity

Energy input = Energy loss at thermal equilibrium

Energy input — excess energy in an electron liberated in a photoionization;  $\frac{1}{2}mv^2 = h(\nu - \nu_0)$

Energy loss — (i) recombination, removing  $\frac{1}{2}mv^2$   
(ii) free-free emission  
(iii) collisionally excited line radiation

## Energy input by photoionization

$$G(H) = N_{H^0} \int_{\nu_0}^{\infty} \frac{4\pi J_\nu}{h\nu} h(\nu - \nu_0) \alpha_\nu (H^0) d\nu$$

at ionization equilibrium

$$N_{H^0} \int_{\nu_0}^{\infty} \frac{4\pi J_\nu}{h\nu} \alpha_\nu d\nu = N_e N_p \alpha_A (H^0, T)$$

(2)

$$\text{therefore } G(H) = N_e N_p \alpha_A(H^o, T) \frac{\int_{\nu_0}^{\infty} \frac{J_{\nu}}{h\nu} (\nu - \nu_0) \alpha_{\nu}(H^o) d\nu}{\int_{\nu_0}^{\infty} \frac{J_{\nu}}{h\nu} \alpha_{\nu}(H^o) d\nu}$$

$$= N_e N_p \alpha_A(H^o, T) \frac{3}{2} k T_i$$

$$\bar{E} = \frac{1}{2} m \bar{J}^2 = \frac{3}{2} k T_i$$

$T_i$  is the initial temperature of the newly created photoelectrons.

$$\tau_0 = \int_0^r N_{H^o}(r') \alpha_{\nu_0} dr' \quad \text{at threshold } \nu_0$$

TABLE 3.1  
*Mean input energy of photoelectrons*

Model stellar atmosphere $T_*(^o \text{ K})$	$T_i(^o \text{ K})$			
	$\tau_0 = 0$	$\tau_0 = 1$	$\tau_0 = 5$	$\tau_0 = 10$
$3.0 \times 10^4$	$1.46 \times 10^4$	$1.81 \times 10^4$	$3.61 \times 10^4$	$5.45 \times 10^4$
$3.5 \times 10^4$	$2.15 \times 10^4$	$2.65 \times 10^4$	$4.67 \times 10^4$	$6.31 \times 10^4$
$4.0 \times 10^4$	$2.67 \times 10^4$	$3.38 \times 10^4$	$6.52 \times 10^4$	$9.57 \times 10^4$
$5.0 \times 10^4$	$3.50 \times 10^4$	$4.47 \times 10^4$	$8.47 \times 10^4$	$11.87 \times 10^4$

## Energy loss by recombination

$$L_R(H) = N_e N_p k T \beta_A(H^o, T)$$

where  $\beta_A(H^o, T) = \sum_{n=1}^{\infty} \sum_{L=0}^{n-1} \beta_{nL}(H^o, T)$

with  $\beta_{nL}(H^o, T) = \frac{1}{kT} \int_0^{\infty} v \sigma_{nL}(H^o, T) \frac{1}{2} m v^2 f(v) dv$

$\beta_{nL}$ : a kinetic-energy-averaged recombination coefficient

As  $\sigma \propto v^{-2}$ , electrons of lower kinetic energy are preferentially captured, and the mean energy of the captured electrons is somewhat lower than  $\frac{3}{2} kT$ .

For a pure H nebula, with no radiation loss

$$G(H) = L_R(H) \Rightarrow \text{gives } T, \text{ and } T > T_i$$

For a H + He nebula, with no radiation loss

$$G(H) + G(He) = L_R(H) + L_R(He)$$

Heating and recombination cooling rates are proportional to the densities of the ions, so heavy elements are not important contributors of these rates.

(4)

## Energy Loss by Free-Free Radiation

Spitzer §3.5

free-free transitions of electrons in encounters  
with positive ions  $\rightarrow$  bremsstrahlung

Emission coefficient  $j_\nu$

$$\begin{aligned} j_\nu &= \frac{8}{3} \left(\frac{2\pi}{3}\right)^{\frac{1}{2}} \frac{Z^2 e^6}{m_e^{3/2} c^3 (\hbar T)^{1/2}} g_{ff} N_e N_i e^{-h\nu/kT} \\ &= 5.44 \times 10^{-39} \frac{g_{ff} Z^2 N_e N_i}{T^{1/2}} e^{-h\nu/kT} \text{ erg cm}^{-3} \text{s}^{-1} \text{sr}^{-1} \text{H}_2^{-1} \end{aligned}$$

where  $g_{ff}$  is the Gaunt factor,

$$g_{ff} = \frac{3^{1/2}}{\pi} \left[ \ln \frac{(2kT)^{3/2}}{\pi e^2 v m_e} - \frac{5\gamma}{2} \right]$$

where  $\gamma$  is the Euler's constant = 0.577.

Cooling rate  $L_{FF}(z) = \int 4\pi j_\nu d\nu$

$$= \frac{2^5 \pi e^6 z^2}{3^{3/2} h m_e c^3} \left( \frac{2\pi kT}{m_e} \right)^{1/2} \langle g_{ff} \rangle N_e N_i$$

$$= 1.42 \times 10^{-27} Z^2 T^{1/2} \langle g_{ff} \rangle N_e N_i$$

The mean Gaunt factor  $\langle g_{ff} \rangle$  is in the range 1.0 - 1.5 for general nebular conditions.

(5)

## Energy Loss by Collisionally Excited Line Radiation

At  $10^4 \text{ K}$ ,  $kT = 0.86 \text{ eV}$ . The K.E. of an electron is high enough to excite the ground levels of common ions, but not H and He.

1 H						2 He
3 Li	4 Be	5 B	6 C	7 N	8 O	9 F
11 Na	12 Mg	13 Al	14 Si	15 P	16 S	17 Cl
						10 Ne
						18 Ar

$$\text{Energy level : } {}^{2S+1}L_J$$

Depending on the number of p electrons, the energy levels are split differently.

$p^1$  and  $p^5$  have similar energy level diagrams

$p^2$  and  $p^4$  " " " " "

Examples:  $p^1$  -  $C^+$ ,  $N^{+2}$ ,  $O^{+3}$ ,  $S^{+3}$

$p^2$  -  $C$ ,  $N^+$ ,  $O^{+2}$ ,  $Si$ ,  $S^{+2}$

$p^3$  -  $N$ ,  $O^+$ ,  $Ne^{+3}$ ,  $S^+$

$p^4$  -  $O$ ,  $Ne^{+2}$ ,  $S$

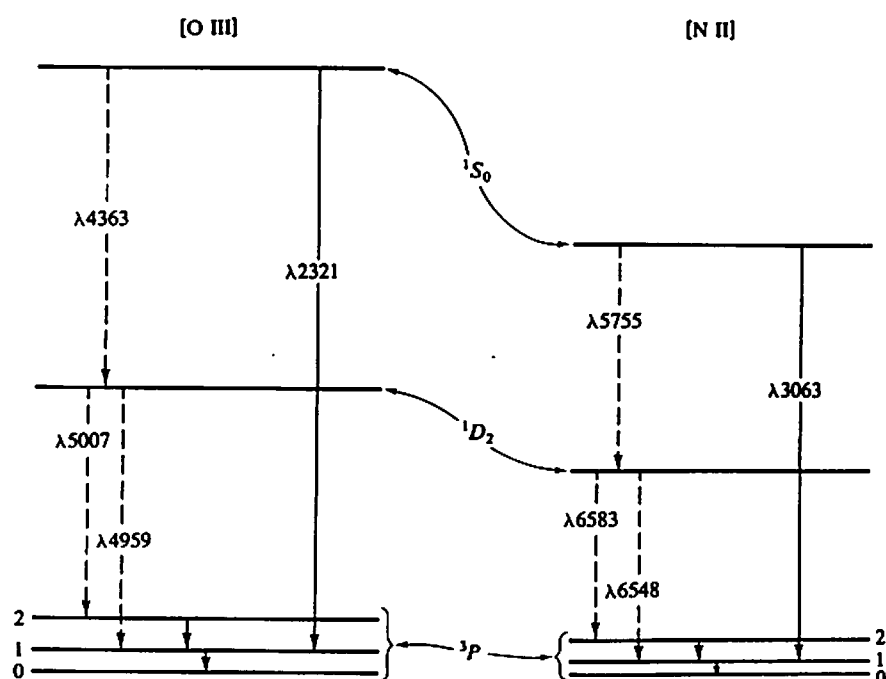
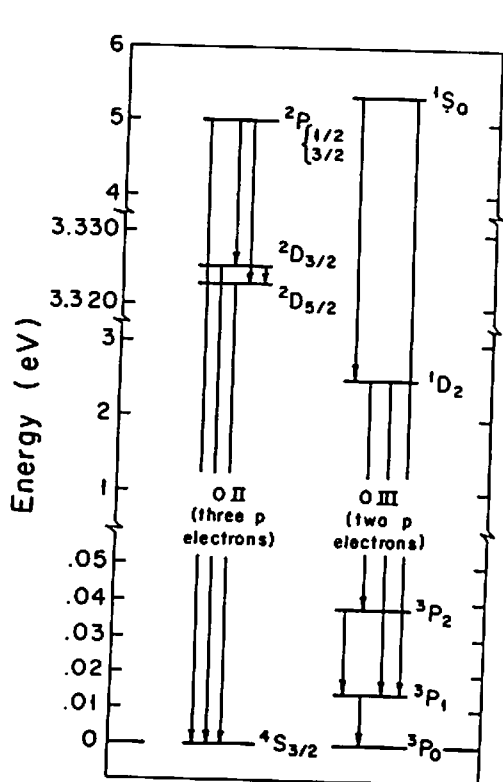
$p^5$  -  $Ne^+$ ,  $Ar^+$

(6)

$$p^1 \quad L=1 \quad \left. \begin{array}{l} \\ S=\frac{1}{2} \end{array} \right\} \quad J=\frac{1}{2}, \frac{3}{2} \Rightarrow {}^2P_{1/2}, {}^2P_{3/2}$$

$$p^2 \quad L=0, 1, 2 \quad \left. \begin{array}{l} \\ S=0, 1 \end{array} \right\} \Rightarrow {}^1S_0 \quad {}^3P_0, {}^3P_1, {}^3P_2 \quad {}^1D_2$$

$$p^3 \quad L=0, 1, 2 \quad \Rightarrow \quad {}^4S_{3/2} \quad {}^2P_{1/2}, {}^2P_{3/2} \quad {}^2D_{3/2}, {}^2D_{5/2}$$

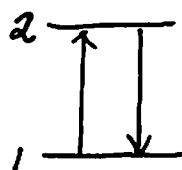


Energy level diagrams for  $O^{+2}$  and  $N^+$

(Osterbrock, Fig 3.1)

Energy level diagrams  
for  $O^+$ ,  $O^{+2}$   
(Spitzer, Fig 4.1)

(7)



$$\Delta E = \chi$$

collisionally excited from level 1  
to level 2

The cross section of excitation  $\sigma_{1,2}(v)$

$$\sigma_{1,2}(v) = 0 \quad \text{for } \frac{1}{2}mv^2 < \chi$$

$$\sigma_{1,2}(v) = \frac{\pi \hbar^2}{m^2 v^2} \frac{\Omega(1,2)}{\omega_1} \quad \text{for } \frac{1}{2}mv^2 > \chi$$

where  $\Omega(1,2)$  is the collisional strength  
and is a function of  $v$   
 $\omega_1$  is the statistical weight of level 1

A free electron with velocity  $v_1$  collides with the ion at level 1 and excites the ion to level 2. The final velocity of the electron is  $v_2$ .

$$\begin{aligned} \frac{1}{2}mv_1^2 &= \frac{1}{2}mv_2^2 + \chi \\ \Rightarrow v_1 dv_1 &= v_2 dv_2 \end{aligned}$$

According to the principle of detailed balancing,  
in thermodynamic equilibrium each microscopic  
process is balanced by its inverse; therefore

$$N_e N_1 v_1 \sigma_{1,2}(v_1) f(v_1) dv_1 = N_e N_2 v_2 \sigma_{2,1}(v_2) f(v_2) dv_2$$

Using Boltzmann equation:  $\frac{N_2}{N_1} = \frac{\omega_2}{\omega_1} e^{-\chi/kT}$

(8)

$$\text{Maxwell-Boltzmann} \quad f(v) = \frac{4}{\sqrt{\pi}} \left( \frac{m}{2kT} \right)^{3/2} v^2 e^{-mv^2/2kT}$$

$$\omega_1 v_1^2 e^{-mv_1^2/2kT} \sigma_{12}(v_1) = \omega_2 e^{-\Omega(1,2)} v_2^2 e^{-mv_2^2/2kT} \sigma_{21}(v_2)$$

$$\Rightarrow \omega_1 v_1^2 \sigma_{12}(v_1) = \omega_2 v_2^2 \sigma_{21}(v_2)$$

$$\begin{aligned} \sigma_{21}(v_2) &= \frac{\omega_1}{\omega_2} \frac{v_1^2}{v_2^2} \sigma_{12}(v_1) \\ &= \frac{\omega_1}{\omega_2} \frac{v_1^2}{v_2^2} \frac{\pi \hbar^2}{m^2 v_1^2} \frac{\Omega(1,2)}{\omega_1} \\ &= \frac{\pi \hbar^2}{m^2 v_2^2} \frac{\Omega(1,2)}{\omega_2} \end{aligned}$$

Collisional strengths are symmetrical in 1 and 2.  
 $\Omega(1,2) = \Omega(2,1)$

Collisional de-excitation rate is ( $\text{cm}^{-3} \text{s}^{-1}$ )

$$\begin{aligned} N_e N_2 \gamma_{21} &= N_e N_2 \int_0^\infty v \sigma_{21}(v) f(v) dv \\ &= N_e N_2 \frac{\pi \hbar^2}{m^2 \omega_2} \frac{4}{\sqrt{\pi}} \left( \frac{m}{2kT} \right)^{3/2} \int_0^\infty v e^{-mv^2/2kT} \Omega(1,2) dv \\ &= N_e N_2 \left( \frac{2\pi}{kT} \right)^{1/2} \frac{\hbar^2}{m^{3/2}} \frac{\Omega(1,2)}{\omega_2} \\ &= N_e N_2 \frac{8.629 \times 10^{-6}}{T^{1/2}} \frac{\Omega(1,2)}{\omega_2} \end{aligned}$$

if  $\Omega(1,2)$  is a constant.

$$\Omega(1,2) = \int_0^\infty \Omega(1,2; E) e^{-E/kT} d\left(\frac{E}{kT}\right), \quad \text{where } E = \frac{1}{2} m v_2^2$$

Collisional excitation rate is

$$N_e N_i g_{12} = N_e N_i \frac{8.629 \times 10^{-6}}{T^{1/2}} \frac{\Omega(1,2)}{\omega_i} e^{-E/kT}$$

The collisional strengths ( $\Omega$ ) must be calculated quantum-mechanically. Osterbrock's Tables 3.3 through 3.7 give numerical values of collisional strengths of important ions.

$$\begin{aligned} \text{Statistical weight for } SL &= (2S+1)(2L+1) \\ \text{''} &\quad \text{for } SLJ = (2J+1) \end{aligned}$$

$$\Omega(SLJ, S'L'J') = \frac{2J'+1}{(2S'+1)(2L'+1)} \Omega(SL, S'L')$$

### Radiative de-excitation

Spontaneous radiative transition probability  
→ Einstein A's

Selection rules for permitted transitions:

- (1) Electron configuration must change by 1 orbital  
 $2p^4 \rightarrow 2p^3 3d^1$     permitted  
 $\rightarrow 2p^4$                     forbidden
- (2)  $\Delta J = 0, \pm 1$ , but not  $J = 0 \rightarrow 0$
- (3)  $\Delta S = 0$
- (4)  $\Delta L = 0, \pm 1$

The more rules are violated, the smaller the transition probability.

(10)

The transition probabilities of  $p^2$ ,  $p^3$ , and  $p^4$  ions are tabulated in Osterbrock's Tables 3.8, 3.9, and 3.10.

For a 2-level ion, if equilibrium is established between the two levels, excitation rate = de-excitation rate.

$$N_e N_1 g_{12} = N_e N_2 g_{21} + N_2 A_{21}$$

$$\frac{N_2}{N_1} = \frac{N_e g_{12}}{A_{21}} \left[ \frac{1}{1 + N_e g_{21}/A_{21}} \right]$$

$$\text{Cooling rate } L_c = N_2 A_{21} h\nu_{21}$$

$$= N_e N_1 g_{12} h\nu_{21} \left[ \frac{1}{1 + N_e g_{21}/A_{21}} \right]$$

at low-density limit,  $N_e \rightarrow 0$

$$L_c \approx N_1 g_{12} h\nu_{21}$$

at high-density limit,  $N_e \rightarrow \infty$

$$\begin{aligned} L_c &\approx N_1 A_{21} h\nu_{21} \frac{g_{12}}{g_{21}} \\ &= N_1 \frac{\omega_2}{\omega_1} e^{-\chi/kT} A_{21} h\nu_{21} \end{aligned}$$

the thermodynamic-equilibrium cooling rate.

Most ions are more complex. For example, all ions with ground configurations  $p^2$ ,  $p^3$ , or  $p^4$  have 5 low-lying levels.

For a 5-level ion, equilibrium equations are

$$\sum_{j \neq i} N_j N_e g_{ji} + \sum_{j > i} N_j A_{ji} = \sum_{j \neq i} N_i N_e g_{ij} + \sum_{j < i} N_i A_{ij}$$

for each of the levels  $i = 1 - 5$

$$\sum_j N_j = N \quad \text{is the total number of ions.}$$

Solve the relative population in each level, then collisionally excited radiative cooling rate

$$L_c = \sum_i N_i \sum_{j < i} A_{ij} h \nu_{ij}$$

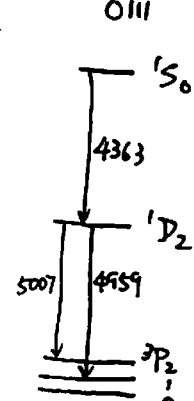
Critical density  $N_c(i)$  is defined to be

$$N_c(i) = \frac{\sum_{j < i} A_{ij}}{\sum_{j \neq i} g_{ij}}$$

electron density at which collisional de-excitations are as important as radiative de-excitation.

Osterbrock  
Table 3.11  
For  $T = 10^4 K$

Ion	Level	$N_c(\text{cm}^{-3})$	Ion	Level	$N_c(\text{cm}^{-3})$
C II	$^2P_{3/2}$	$8.5 \times 10^1$	O III	$^1D_2$	$7.0 \times 10^5$
	$^3P_2$	$5.4 \times 10^5$	O III	$^3P_2$	$3.8 \times 10^3$
N II	$^1D_2$	$8.6 \times 10^4$	O III	$^3P_1$	$1.7 \times 10^3$
	$^3P_2$	$3.1 \times 10^2$	Ne II	$^2P_{1/2}$	$6.6 \times 10^5$
N II	$^3P_1$	$1.8 \times 10^2$	Ne III	$^1D_2$	$7.9 \times 10^6$
	$^2P_{3/2}$	$3.2 \times 10^3$	Ne III	$^3P_0$	$2.0 \times 10^4$
N III	$^3P_2$	$1.4 \times 10^6$	Ne III	$^3P_1$	$1.8 \times 10^5$
O II	$^2D_{3/2}$	$1.6 \times 10^4$	Ne V	$^1D_2$	$1.6 \times 10^7$
O II	$^2D_{5/2}$	$3.1 \times 10^3$	Ne V	$^3P_2$	$3.8 \times 10^5$
			Ne V	$^3P_1$	$1.8 \times 10^5$



(12)

## Resulting Thermal Equilibrium

$$G = L_R + L_{FF} + L_c$$

$$G \propto N_e N_p$$

$$L_{FF} \propto N_e N_i$$

$$L_c \propto N_e N_i \quad \text{at low-density limit}$$

$$\propto N_i \quad \text{at high-density limit}$$

At low-density limit, the resulting temperature is dependent on the abundances of heavy elements, but is not dependent on density.

At high-density limit, the collisionally excited radiative loss is decreased, resulting in a higher equilibrium temperature.

Example:

$$\frac{N(O)}{N(H)} = 7 \times 10^{-4}, \quad \frac{N(Ne)}{N(H)} = 9 \times 10^{-5}, \quad \frac{N(N)}{N(H)} = 9 \times 10^{-5}$$

assuming O, Ne, N are all 80% singly ionized  
20% doubly ionized.

H is 0.1% neutral, 99.9% ionized.

Radiative cooling peaks at  $kT \approx \chi$

Results: Figure 3.2 for low  $N_e$ , Figure 3.3 for  $N_e = 10^4 \text{ cm}^{-3}$

Effective heating rate =  $G - L_R = L_{FF} + L_c = \text{effective cooling rate.}$

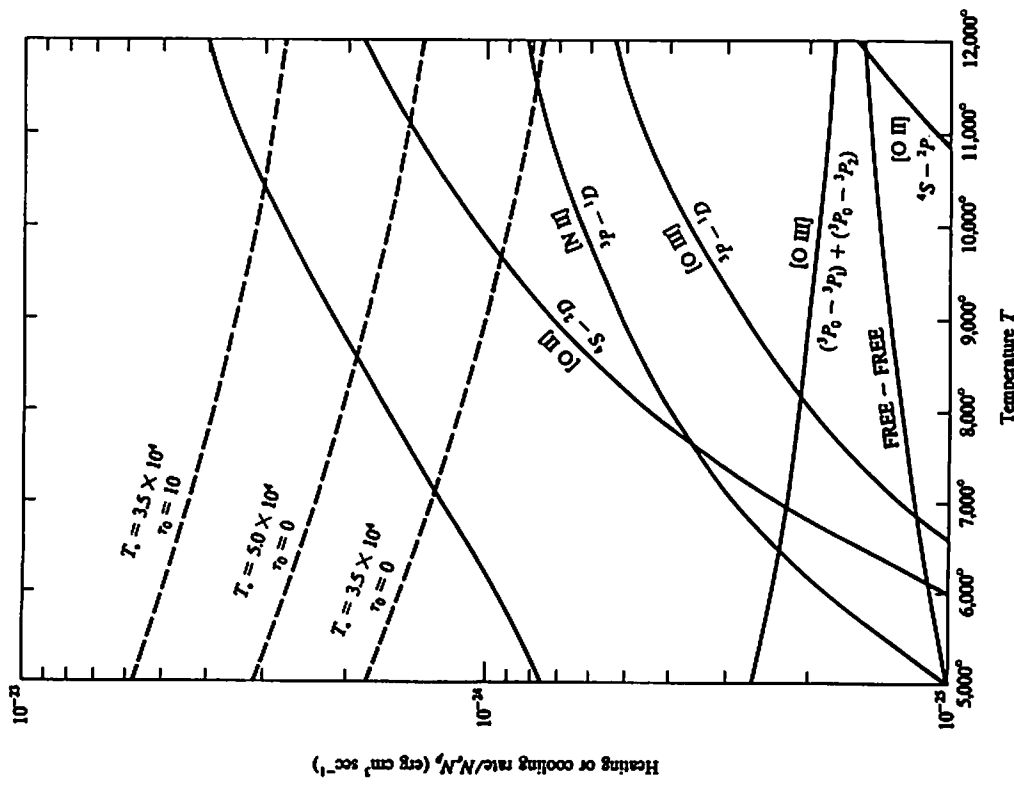


FIGURE 3.2  
Net effective heating rates ( $G - L_R$ ) for various stellar input spectra, shown as dashed curves. Total radiative cooling rate ( $L_{FF} + L_C$ ) for the simple approximation to the H II region described in the text is shown as highest solid black curve, and the most important individual contributors to radiative cooling are shown by labeled solid curves. The equilibrium temperature is given by the intersection of a dashed curve and the highest solid curve. Note how the increased optical depth  $\tau_0$  or increased stellar temperature  $T_0$  increases  $T_e$  by increasing  $G$ .

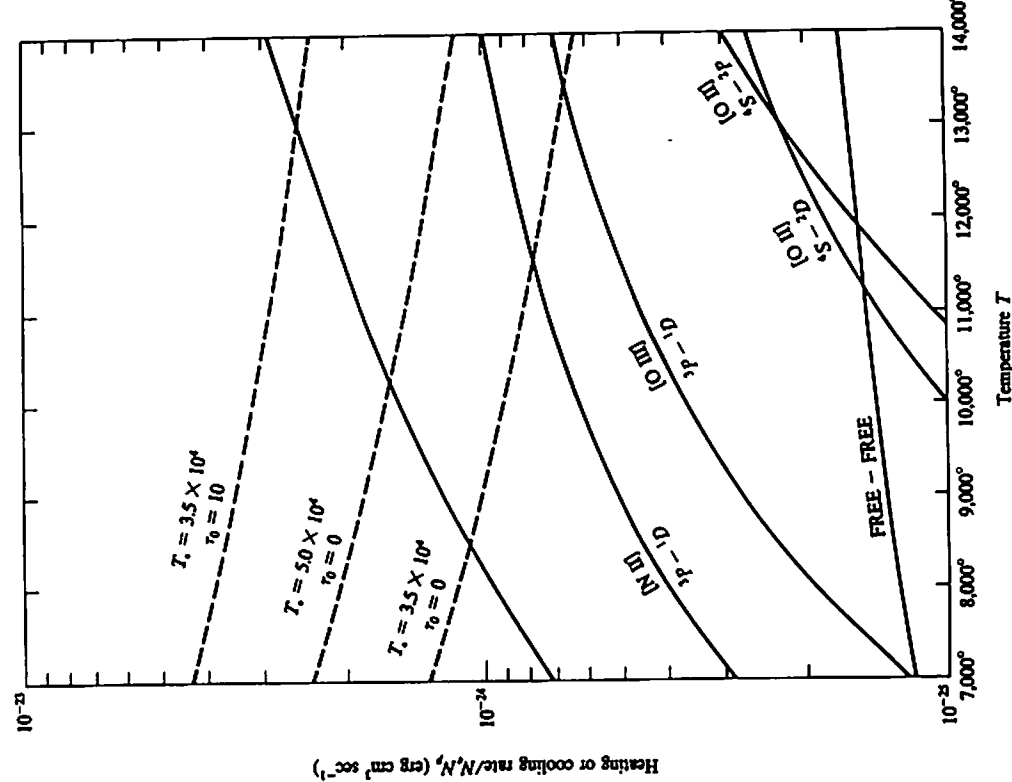


FIGURE 3.3  
Same as Figure 3.2, except that collisional de-excitation at  $N_e = 10^4 \text{ cm}^{-3}$  has been approximately taken into account in the radiative cooling rates.

13

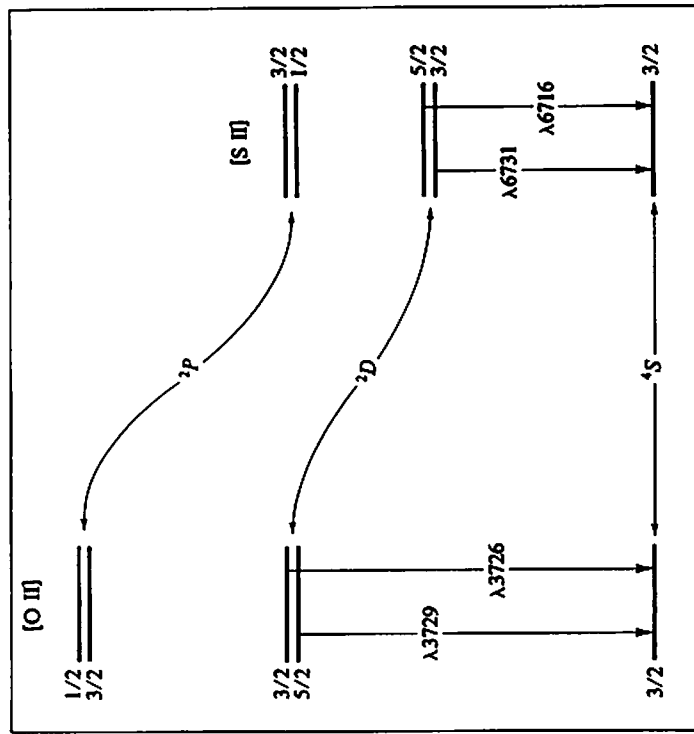
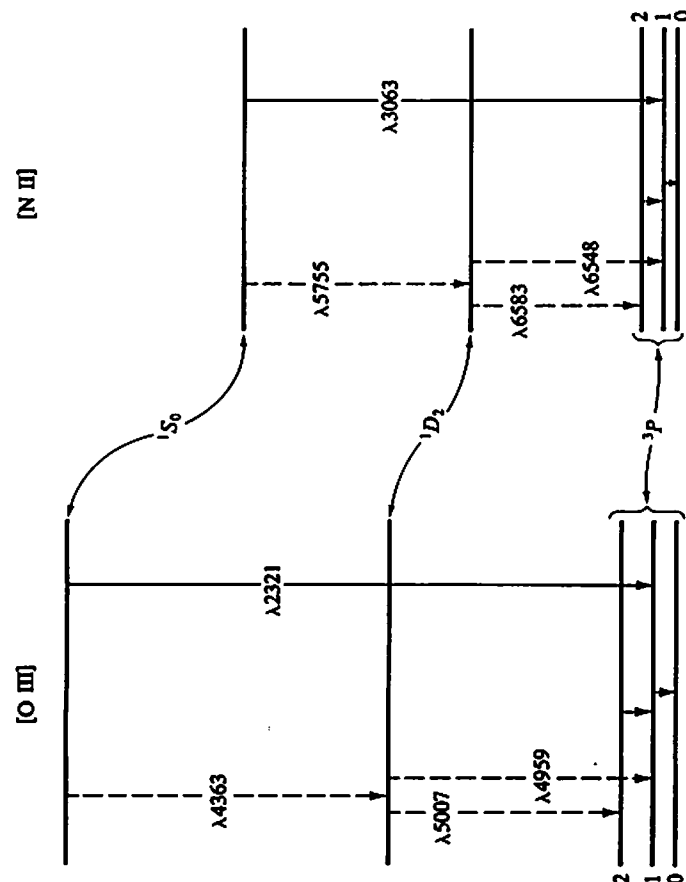


FIGURE 3.1  
Energy-level diagram for lowest terms of [O III], all from ground  $2p^2$  configuration, and for [N II], of the same iso-electronic sequence. Splitting of the ground  $3P$  term has been exaggerated for clarity. Emission lines in the optical region are indicated by dashed lines, and by solid lines in the infrared and ultraviolet. Only the strongest transitions are indicated.

FIGURE 5.2  
Energy-level diagrams of the  $2p^3$  ground configuration of [O II] and  $3p^3$  ground configuration of [S II].